Proceedings of the ASME 2013 International Mechanical Engineering Congress & Exposition
IDETC/CIE 2013
November 15-21, 2013, San Diego, USA

DRAFT IMEC2013-64387

SIMPLIFIED THERMO-ELASTOPLASTIC NUMERICAL MODELLING TECHNIQUES APPLIED TO FRICTION STIR WELDING OF MILD STEEL

Daniel Micallef
Mechanical Engineering Department
University of Malta
Tal-Qroqq, Msida, Malta, MSD2080
Email: daniel.micallef@um.edu.mt

Duncan Camilleri*
Mechanical Engineering Department
University of Malta
Tal-Qroqq, Msida, Malta, MSD2080
Email: duncan.camilleri@um.edu.mt

Pierluigi Mollicone
Mechanical Engineering Department
University of Malta
Tal-Qroqq, Msida, Malta, MSD2080
Email: pierluigi.mollicone@um.edu.mt

ABSTRACT

Friction stir welding is a relatively new advanced joining technique that requires minimal power input, ultimately leading to less inherent residual stresses and distortion. The process involves a spinning tool which first plunges into the surface of the, to be welded assembly and then traverses along the joint. Frictional heat is generated, softening the material at temperatures significantly below the melting temperature of the parent material. As the tool traverses along the joint at a predetermined speed, the assembly is joined by means of a plastic straining process. This advanced welding technology has been validated for various aluminium alloys but it is only recently, due to advances in tool technology, that the possibility of joining mild steel using friction stir welding has become a viable option. This study looks into friction stir welding of mild steel and develops simplified numerical methods for the prediction of thermal gradients, residual stresses and deformation. In principle the process modelling requires a multi-disciplinary approach involving coupled thermo-fluid, microstructural-structural modelling process. Much of the latest thermo-mechanical studies of friction stir welding rely on a number of over simplifications particularly related to the heat flux distribution across the tool shoulder, and also on the backing plate boundary conditions. The objective of this paper is to scrutinise the effects of modelling in more detail and establish the most important factors leading to accurate yet computationally efficient prediction of thermal gradients and inherent residual stresses. The results show that both the heat input and heat loss modelling, due to heat dissipation to the surroundings, are crucial for the determination of the final inherent welding residual stresses. The heat generated is modelled through a predefined linear heat flux variation across the tool shoulder. However if a more precise and localized residual stress information is sought, a full thermo-fluid-structural analysis is required. This is time consuming and probably does not give significant information on manufacturing optimization. On the other hand, simplified global solutions offer the possibility to optimise friction stir welding parameters and boundary conditions during the preliminary stages of the development of the fabrication procedures, at relatively minimal time and processing power. This work is financed under the European Commission in Call FP7-SST-2012-RTD-1 High Integrity Low Distortion Assembly (HILDA) project

NOMENCLATURE

Q_{total} Total heat input [W].
Q_s Heat input by the tool shoulder [W].
Q_p Heat input by the tool pin [W].
μ Tool-workpiece friction coefficient.
N Tool rotational speed [RPS].
p Tool pressure [Pa].
R_s Tool shoulder radius [m].
R_p Tool pin radius [m].
h Tool height [m].
q'' Heat flux from tool shoulder [W/m^2].
q''' Volumetric heat generation from tool pin[W/m^3].

*Address all correspondence to this author.

T Temperature [^oC].
σ_x Residual stress along the longitudinal direction [Pa].
σ_z Residual stress along the transverse direction [Pa].

INTRODUCTION

Overview of the friction stir welding process

The Friction Stir Welding (FSW) process was invented by The Welding Institute (TWI) in 1991 [1]. When it was invented, its application was limited to aluminium but is nowadays also being considered for the welding of various types of materials. FSW is a solid-state joining process, since in principle no melting occurs in the parent material. Rather, the material is plasticized in such a way that it deforms and flows past a rotating tool. The plasticizing action is attained due to the frictional heat and shear deformation generated by the rotating tool. A schematic representation of the process is shown in Fig. 1.

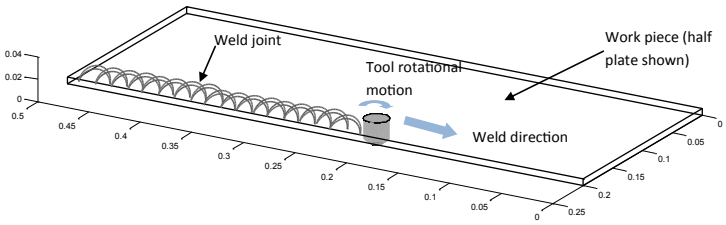

FIGURE 1. SCHEMATIC OF THE FRICTION STIR WELDING PROCESS.

A schematic of the tool is also shown in Fig. 2. Further information on the principles of FSW process can be found in the book by Mishra & Mahoney [2].

The process starts by plunging the tool into the material until contact is established between the tool shoulder surface and the assembly. In order to ensure that the material is sufficiently softened, the tool is left to dwell for some time (referred to the dwell period), before it is traversed along the joint. The heating process occurs primarily due to friction but also due to the plastic deformation of the material. Much of the interest in FSW is that it creates a fully re-crystallized, equiaxed and fine grained microstructure which promotes excellent mechanical and fatigue properties. In addition, it is well known that the distortion resulting in the work piece after the welding process is minimal compared to for instance fusion welding. The study conducted by McPherson et al. [3] compares submerged arc welding with FSW of DH36 and shows that FSW gives significant enhancement in toughness and fatigue properties. However they claim that at this stage the cost incurred due to tool wear are relatively high. This could perhaps be the main reason why little research was focused on

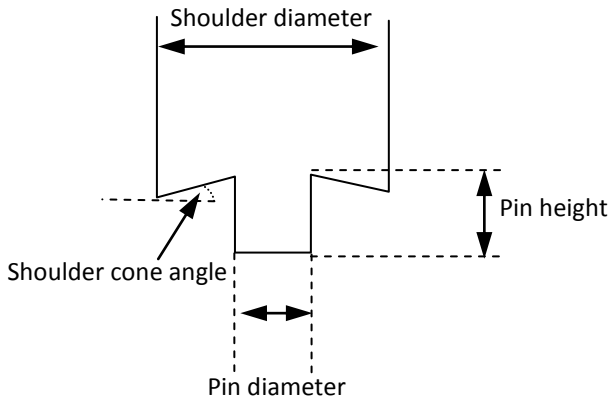

FIGURE 2. TYPICAL TOOL GEOMETRY AND IMPORTANT DIMENSIONS.

FSW of mild steel. Current research is focused on reducing the tool wear making FSW of mild steel a more viable welding technique. The use of numerical modelling will certainly help to attain this by understanding and establishing the main parameters affecting FSW, consequently leading to optimisation.

State of the art - numerical modelling

FSW is a multi-physics problem and as such requires the modelling of different physical phenomena. To date, there are limited models which are able to solve the coupled thermo-fluid-structural equations characterising FSW. Research has been mainly focused on either the thermal, flow or structural behaviour individually, in an uncoupled fashion. In the study conducted by Fratini et al. [4] a simplified uncoupled approach was adopted where the thermal gradients predicted from a thermal FEA simulation are calculated first. The results are then inputted into the structural FEA model in the form of thermal loads. The same approach has also been utilized in the past for example by Soundararajan et al. [5], Staron et al. [6] and Riahi et al. [7] in order to analyze the thermo-structural behaviour of friction stir welded aluminium alloys.

More recently the interest in applying FSW to steels has increased. When compared to the FSW of aluminium, minimal research effort has been conducted to understand the mechanics behind FSW of steels. Only, a few examples of such studies exist in literature, for example that of Zhu et al. [8] where a thermo-elastoplastic FSW numerical model is carried out. Effects due to heat sinks are largely ignored.

A complete review of the numerical modelling of the FSW process is given by D. Neto and P. Neto [9]. An overview of fundamental research in the various fields associated with FSW is given hereunder.

Thermal modelling The most challenging part in the thermal modelling is the correct specification of the heat generated due to friction and plastic deformation, together with the boundary conditions. Riahi et al. [7] defined the heat input due to FSW as the sum of the heat generated at the pin and at the shoulder region of the tool:

$$Q_{total} = Q_s + Q_p \tag{1}$$

Where Q_s is the heat input from the shoulder,

$$Q_s = \frac{4\pi^2}{3}\mu N p(R_s^3 - R_p^3) \tag{2}$$

and Q_p is the heat input from the tool pin,

$$Q_p = \frac{4\pi^2}{3}\mu N p(R_s^3 - 3R_p^2 h) \tag{3}$$

where μ is the friction coefficient of the tool to work piece contact, N is the rotational speed of the tool in revolutions per second, p is the pressure, R_s is the tool shoulder radius, R_p is the tool pin radius and h is the tool pin height. The total heat input is hence given by

$$Q_{total} = \frac{4\pi^2}{3}\mu N p(R_s^3 + 3R_p^2 h) \tag{4}$$

A more detailed analytical approach can be found in the study conducted by Schmidt et al. [10]. The authors consider three contact states during the process namely:

1. *Sliding*: where the contact shear stress is smaller than the material yield shear stress.
2. *Sticking*: where the contact shear stress is larger than the material yield shear stress. In this case the material sticks and is transported with the moving tool surface.
3. *Partial sliding/sticking*: This occurs when the contact shear stress is equal to the material yield shear stress.

With this analytical approach it was possible to establish the contributions of the shoulder, the pin side and the pin tip to the total heat transfer. The shoulder contributes circa 86% of the total heat transfer, 11% is generated at the probe side while the probe tip contributes just 3%. At this stage no dissipation into the tool was not taken into account. Schidmt et al. [11] enhanced their analysis by further including the presence of heat extraction from the tool and other clamping condition. Another study, found in literature, that takes into account heat loss and dissipation is that of Simar et. al. [12] In both cases the models where applied to FSW of aluminium. The situation for the welding of steels needs to be thoroughly scrutinised not only in terms of the heat transferred to the tool but also in the bed and in the clamps. This supports the need for the research questions put forward in this work.

Structural modelling The primary driving forces leading to residual stresses and ultimately distortion, are the thermal strains. These are a result of the thermal loads developed during FSW and the materials tendency to expand and subsequently contract due to the presence of thermal gradients. The expansion and contraction is directly correlated to the coefficient of expansivity that is in turn a function of the microstructural evolution. Though in FSW no melting occurs, temperatures in the region of 1000^oC are often developed at the weld nugget, promoting a phase change to austenite and back to martensite / bainite and pearlite. This generally occurs in a significantly short period of time often promoting a fine grained structure. It is important that such phase change and grain redistribution are somehow captured in the structural model to fully define the residual stresses. A full thermo–microstructural–structural coupled model is required to model this interaction. However, this phenomenon can be uncoupled through the application of appropriate non-linear temperature dependent expansivity properties that take into consideration any volume changes due to phase transformations.

The full prediction of residual stresses and microstructural properties developed due to FSW provides the possibility to assess the toughness and fatigue properties of the weld. For example, compressive residual stresses are well known to promote fatigue properties and corrosion resistance. John et al. [13] and Bussu & Irving [14] have investigated the fatigue performance of friction stir welds and have shown that the welding residual stresses influence the fatigue performance of joints.

Khandkar et al. [15] perform a thermo-mechanical model to investigate the residual stresses developed due to FSW for AA2024, AA6061 and SS304L. For all materials, it was found that the longitudinal stress are the highest and are of prime importance. An uncoupled approach was adopted in all the studies mentioned above.

Hypothesis and research questions

This study develops an uncoupled thermal and structural numerical model applied to FSW of mild steel, in particular DH36. The simplified solution approach allows the determination of heat transferred locally to the tool and to the bed supporting the work piece, which are both expected to be substantial in the FSW of mild steel.

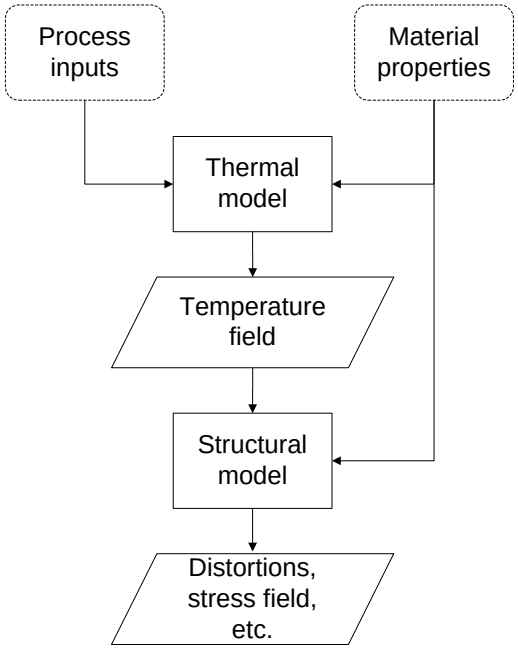

FIGURE 3. FLOWCHART SHOWING THE FEA MODEL WHERE THE TEMPERATURE FIELD FROM THE THERMAL MODEL IS USED AS INPUT TO THE STRUCTURAL MODEL.

The research questions are hence the following:

1. Is a simplified finite element analysis solution adequate for application in manufacturing optimization of the FSW process?
2. Can a simplified solution be used to determine the heat transfers to the tool and to the bed supporting the work piece?
3. Is the heat transferred to the tool and bed of substantial importance?

METHODOLOGY

Numerical approach

The thermal gradients developed during FSW of mild steel are predicted using a transient non-linear temperature dependent thermal model, by means of finite element analysis. The plate is modelled using 3D thermal elements (SOLID70 in ANSYS®) and link elements were used to model the heat transfer (lost) from the plate to the bed and tool. The predicted temperature gradients were then applied as thermal loads to a non-linear structural model, which uses solid structural elements (SOLID185 in ANSYS®).

Fig. 3 gives an overview of the procedure used for the model.

Temperature dependent material properties of shipbuilding DH36 mild steel, including non-linear conduction, specific heat, Youngs modulus, coefficient of expansivity and yield strength properties were applied and established from a previous experimental campaign used to model fusion welding processes [16]. At this stage further research is required to fully characterise the material properties, in particular the coefficient of expansivity as a function of thermal gradients and cooling rates due to FSW. This is highly dependent on the predicted thermal history developed during FSW, which can in turn be highly influenced by the boundary conditions and heat sinks in the vicinity of the weld. As such this firstly requires the predetermination of the temperatures by means of an experimental campaign or through validated numerical models.

Model specifications

The high torque and plunge force associated with FSW requires optimal clamping to ensure that the assembly being welded does not move during welding. Figure4 shows a typical clamping configuration planned to be carried out at TWI. Apart from restraining the assembly, the clamps will act as heat sink altering the thermal gradients developed during welding. In particular the backing plate in conjunction with the machine bed will act as a high thermal absorber. While some heat is extracted from the clamp block, its particular influence is to fully restrain in-plane and out-of-plane movement of the plate. This does not mean that no residual stresses or distortion will ultimately be developed in the work piece. Upon the release of clamping the inherent residual stresses will self-equilibrate with a possibility of developing distortion. Clamping will significantly alter the development of residual stresses and hence must be modelled.

In this study it is assumed that 500mm x 200mm x 6mm plates are friction stir welded. 500mm long plates are considered at this stage to reduce the computational effort. Table 1 shows the material and geometric specification of the work-piece, tool, clamps and machine bed. In this study the initial dwell period is not modelled but the assembly is assumed to reach quasi-static conditions upon weld initiation, according to the welding parameters given in Tab. 2. Furthermore, it is assumed that the heat input is symmetrical and not influenced by the different velocity vectors at the front and rear of the tool, allowing the possibility to model half of the plate.

The heat generated due to FSW is assumed to arise from the friction developed at the tool shoulder and pin as described in Eqns. 2,3 and 4. In the case of the shoulder the heat input is modelled as a heat flux following the linear variation given in eqn. 6

$$q''(r) = \frac{3Q_s r}{2\pi(R_s^3 - R_p^3)} \tag{5}$$

On the other hand the heat developed at the pin tip and sides

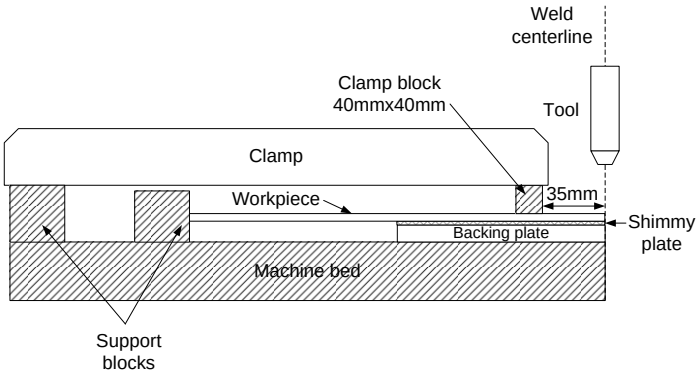

FIGURE 4. SETUP DIAGRAM WHICH IS TO BE MODELLED.

TABLE 1. DIMENSION AND MATERIAL SPECIFICATIONS.

	Dimension	Material
Workpiece plate	2000mmx200mmx6mm	DH36 steel
Tool shoulder radius	11mm	pcBN, Ni, WC composite
Tool pin radius	4mm	pcBN, Ni, WC composite
Tool pin height	5mm	pcBN, Ni, WC composite
Bed height (approx.)	110mm	Cast iron
Backing bar	2000mmx100mmx20mm	O1 steel
Shimmy plate	2000mmx100mmx20mm	Mild steel

are modelled as a volumetric heat generation within the plate elements corresponding to the shape and size of the pin. This heat generated is given by:

$$q''' = \frac{Q_p}{\pi R_p^2 h} \tag{6}$$

Table 3 gives the number of elements used to model the plate including heat sinks, together with the calculated heat input based on the welding parameters given in Tab. 2. Figure 5 shows the mesh used to model the plate. Link elements were used to model the heat sinks and will be described in the following section. Non-linear natural convective and radiation heat transfer coefficients were applied at the surface of the plate that is not in contact with any clamp or shimmy plate (refer to Fig. 6 for boundary conditions and loading configuration). The thermal gradients were predicted using 154 time steps allowing for cooling to ambient temperature of 20^oC in 400s.

TABLE 2. SUMMARY OF THE OPERATING CONDITIONS

Parameter	Quantity
Tool RPM	215RPM
Traverse speed	1.67mm/s
Plunge force	40kN
Friction coefficient	0.6

TABLE 3. SIMULATION SPECIFICATIONS

Number of elements	112868
Number of time steps	154
Cooling time	400s
Ambient temperature	20
Shoulder heat input	3772W
Pin heat input	905W
Total heat input	4677W

In the case of the structural model, it was assumed that the nodes underlying the clamp block are fully restrained. Furthermore the edge of the plate was restrained in the transverse direction. Link elements were used to model the contact between the work piece and the shimmy plate such that any downward movement into the bed is excluded whilst allowing detachment of the plate from the bed. This was done by applying a compressive stiffness but having no tensile stiffness to a suitable link element type. The model was also solved in 154 time steps mimicking that of the thermal model. During the progression of welding a surface load corresponding to the tool plunge force was applied at the shoulder surface. This was sequentially applied along the length of the weld and corresponding to the position of the tool.

Heat sink modelling

Heat sinks are modelled using thermal link elements (LINK33 in ANSYS®). A schematic of the heat sink modelling is shown in Fig. 7. The bed and backing plate heat sink is modelled as a series of thermal resistances consisting of an air gap, shimmy plate, backing plate and bed resistance. At the tool

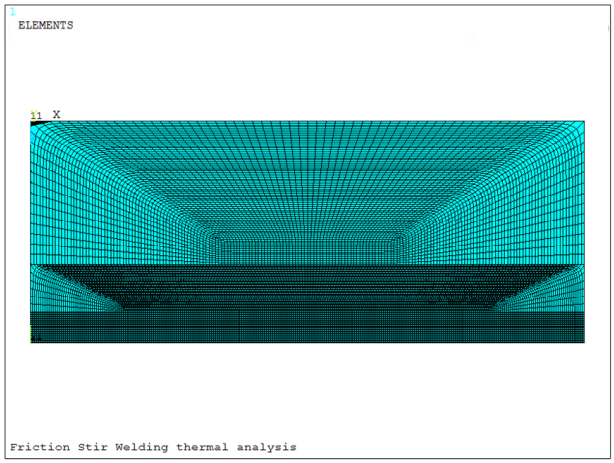

(a) TOP VIEW

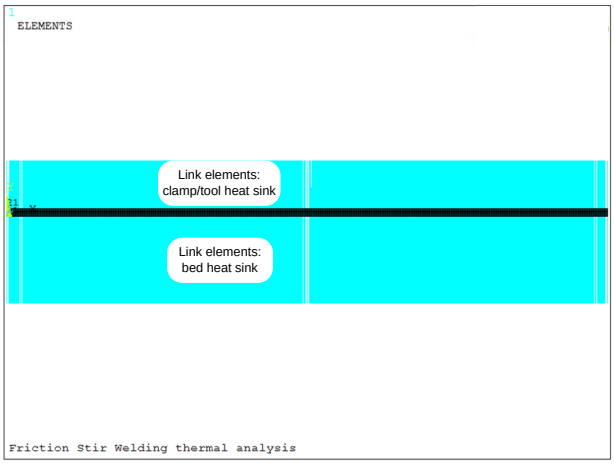

(b) SIDE VIEW

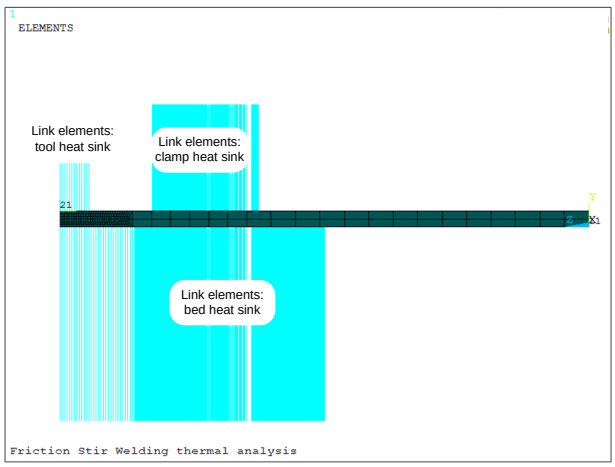

(c) END VIEW

FIGURE 5. DIFFERENT MESH VIEWS

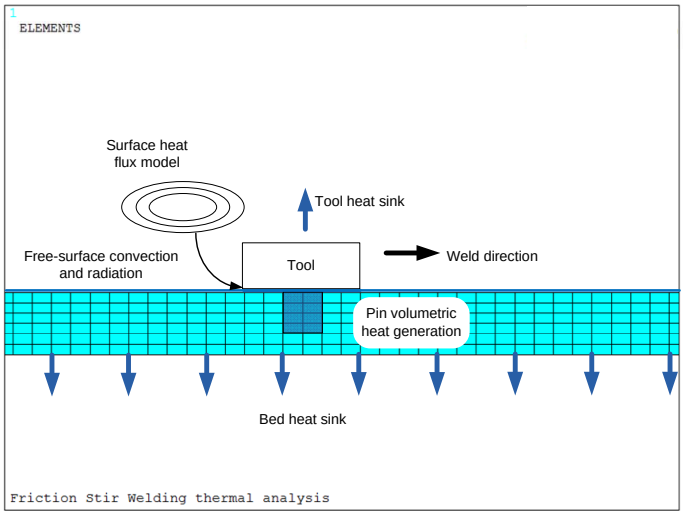

FIGURE 6. BOUNDARY CONDITION SPECIFICATION FOR THE THERMAL FEA MODEL.

location and during the progression of welding, the air-gap resistance was ignored, due to the very good contact between the work piece and the shimmy plate.

The heat sink due to the tool is modelled as a number of thermal resistances distributed over a circular region with radius equal to the tool radius. On the other hand, the clamp block is modelled as a series of links representing the clamp block shown in Fig. 4 and assuming complete contact with the plate. These resistances are also shown in Fig. 7. The values of conductivity used for each of these resistances is given in Tab. 4. Each set of series resistances is added together to reduce the number of link elements that need to be modelled. In all instances an ambient temperature boundary condition was applied at the end of each set of thermal resistances.

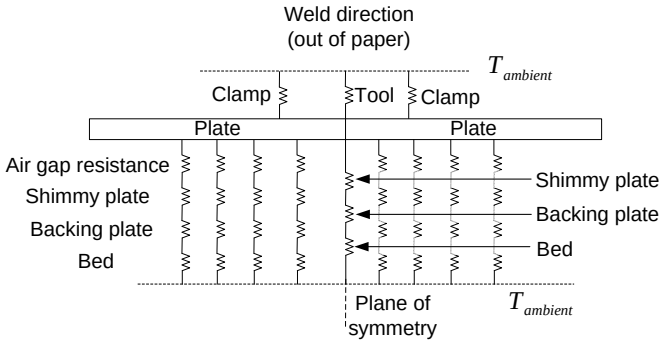

FIGURE 7. MODELLING OF HEAT SINKS.

TABLE 4. CONDUCTIVITY OF MATERIALS USED TO MODEL HEAT SINKS.

Part	Material	Conductivity W/mK
Tool	pcBN, Ni, WC composite	175
Clamp	Mild steel	60.5
Shimmy plate	Mild steel	60.5
Backing plate	O1 steel	32
Bed	Cast iron	55
Contact resistance	Air	0.0257

RESULTS

Temperature profiles

The temperature contour plots show a highly localised temperature at the tool region reaching temperatures of 1000^oC. A high thermal gradient exists in both the transverse and longitudinal direction from the tool region to regions further away from the tool. In a space of a few millimeters the temperature drastically reduces to 300^oC / 400^oC. This is mainly attributed to the heat extracted by the machine bed. Figure 8 shows the temperature profiles predicted by the thermal model towards the end of the weld at 268.7s from the start of the weld (corresponding to a tool location of 448.7mm from the plate start edge). After the tool passes the predominant heat flow is in the transverse direction. Detailed contours are shown in Fig. 9 where the temperature range is changed in Fig. 9(a) and the temperature contours at the tool are shown in detail in Fig. 9(b).

Figure 10 shows the evolution of temperature at the top and bottom surface of the plate for various distances away from the tool centre position. At the tool region and at the top surface temperatures in excess of 800^oC are reached, high enough to plasticize the parent material and promote material stirring. On the other hand a temperature of around 350^oC can be observed at the bottom surface. The temperatures developed away from the tool are comparably low. At these positions the temperatures are relatively linear through the thickness.

Figure 11 shows the temperature distribution through the thickness of the plate at various instances during the welding process. The temperature contours at the tool region are not uniform over the thickness. This is attributed to the non-linear heat input model where the majority of the heat is being developed at the tool shoulder. In fact the temperature at the bottom surface is still relatively low when compared to the top surface. Heat diffusion is rather delayed and the peak temperature at the bottom plate surface continues to increase further as the tool passes. Furthermore a significant amount of heat is being extracted at the bottom surface due to the shimmy plates. This suggests that carefully experimental configuration setup is required to ensure that plastic stirring is also promoted at the bottom surface of the plate, just enough to ensure joining and weld integrity.

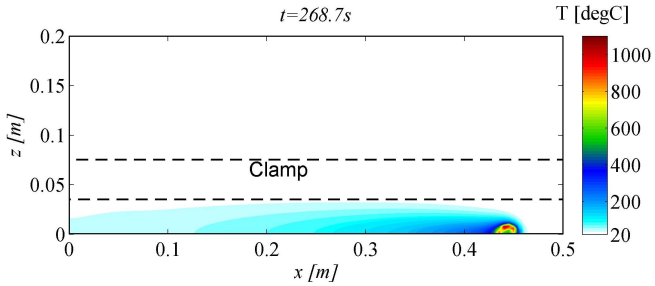

FIGURE 8. TEMPERATURE CONTOUR PLOT SHOWING MEASUREMENT LOCATION.

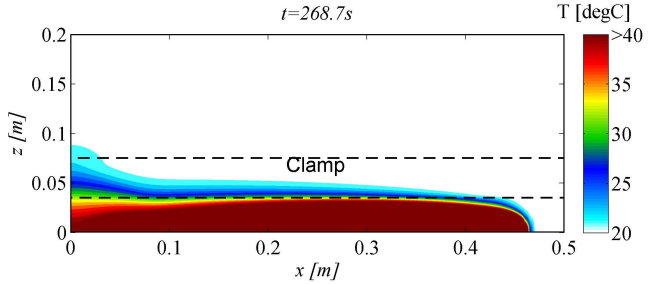

(a) MODIFIED COLOURBAR

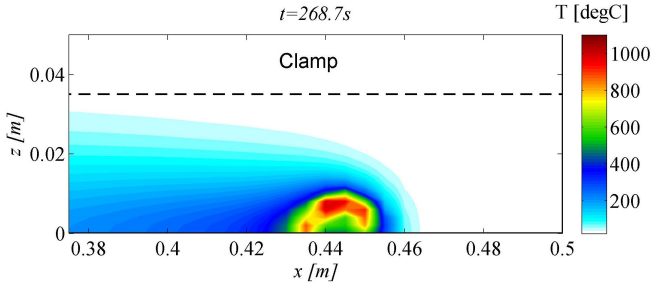

(b) DETAILED TEMPERATURE PROFILES AT THE TOOL

FIGURE 9. DETAILS OF TEMPERATURE CONTOURS

Heat sinks

It is clearly evident that the heat sinks have a significant influence on the predicted temperatures and consequently their effect is discussed in more detail in this section. Figure 12 shows

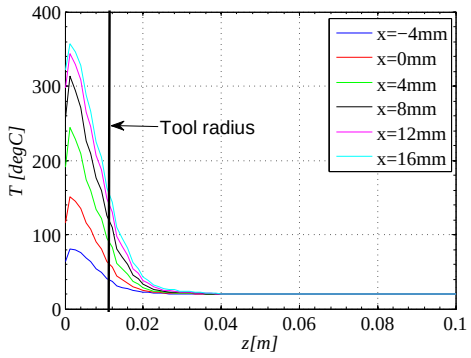

(a) BOTTOM SURFACE

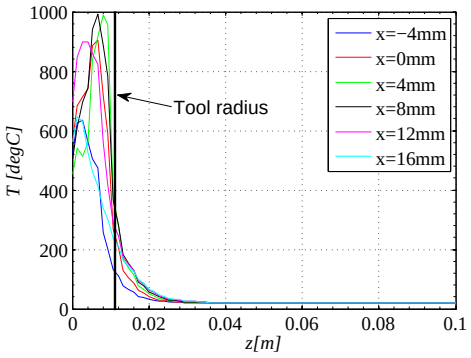

(b) TOP SURFACE

FIGURE 10. TEMPERATURE PROFILE AT THE TOP AND BOTTOM PLATE SURFACES AGAINST THE WIDTH OF THE PLATE AT A DISTANCE OF 0.4487m FROM THE START OF THE WELD.

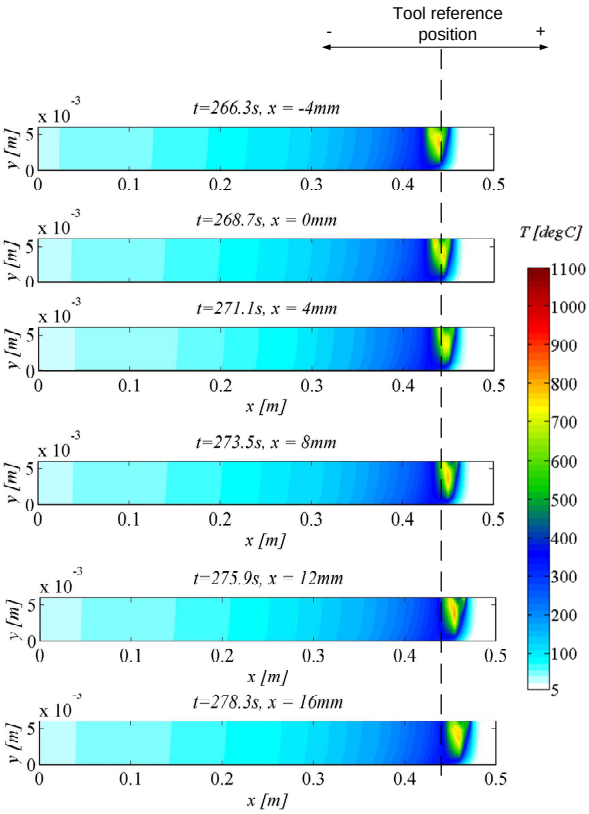

FIGURE 11. TEMPERATURE CONTOUR PLOT ALONG THE THICKNESS OF THE PLATE.

the accumulation of heat dissipation through the bed and the clamp. The heat dissipated through the bed is further divided into two regions (heat dissipated directly underneath the tool and heat dissipated through the rest of the shimmy plate). It is evident that significant heat is lost into the bed, which steadily rises during the welding stage. Underneath the tool the heat loss reaches a steady state just after 20s and remains at a value of around 25W throughout the welding period. Towards the end of the plate the heat dissipated under the tool further increases, but this is a result of the end effects, where higher accumulation of heat is observed. During cooling the gradual reduction in plate temperature to ambient, reduces the amount of heat dissipation and consequently the heat loss decreases rapidly to near zero after 400s from the end of welding. Here no heat loss is considered under the non-present tool.

At face value, Fig. 12 suggests that the heat lost underneath the tool is relatively small. However, when one considers the heat flux, it is clearly evident that the high thermal gradient developed underneath the tool promotes significant and fast cooling. Figure 13 shows the calculated heat flux at various regions during the welding and cooling stages. This suggests that the contact between the plate and bed underneath the tool can have a significant influence on the softening of the weld nugget and should be optimised.

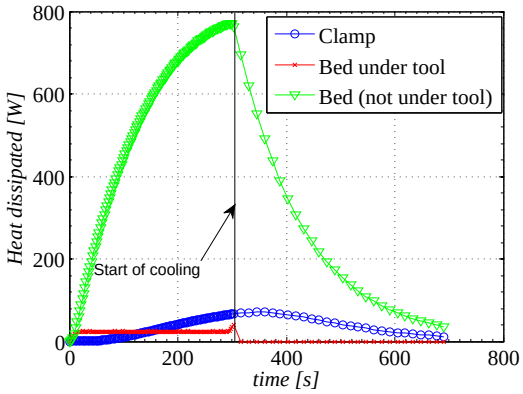

FIGURE 12. HEAT TRANSFER TO THE BED AND CLAMPS WITH TIME.

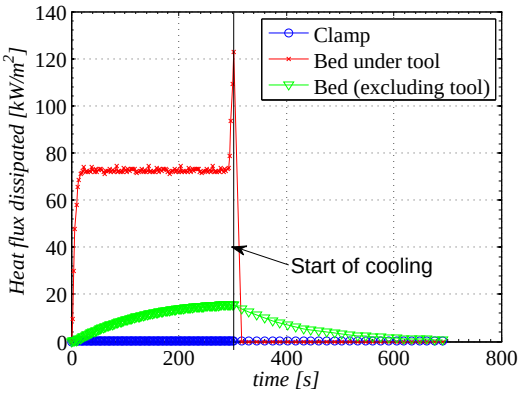

FIGURE 13. HEAT FLUX TO THE BED AND CLAMPS WITH TIME.

Residual stresses

The resulting residual stresses on the top plate surface after cooling are shown in Figs. 14 and 16 for the longitudinal and transverse directions respectively. Both the longitudinal and transverse residual stresses are mainly tensile. At this stage the clamping restraint is still applied, inhibiting the transverse and longitudinal contraction. At the tool region the residual stresses are equivalent to the materials yield limit. In the case of the longitudinal residual stresses this is confined to a space equivalent to the tool radius and slightly beyond. At these points the thermal strains developed in the longitudinal direction during heating process of welding exceed twice yield resulting in permanent plastic deformation. In the case of the transverse residual stresses yielding only occurs at the weld line and a net tensile residual stress of around 250 MPa develops in the region from the plate edge to the clamps. At this point the stress drastically reduces to zero due to the fixed boundary conditions applied. Since yielding is only confined to the weld line, upon removal of the clamps the transverse residual stress will probably reduce to near zero. At this stage the influence of removing the clamps was not investigated but it is envisaged that upon removal of the clamps the residual stresses will self-equilibrate leading to more confined transverse and longitudinal residual stresses when compared to fusion welding and ultimately leading to minimal distortion. Figure 15 and 17 shows the inherent residual stresses developed at the top surface of the plate. The use of clamping significantly alters the development of residual stresses.

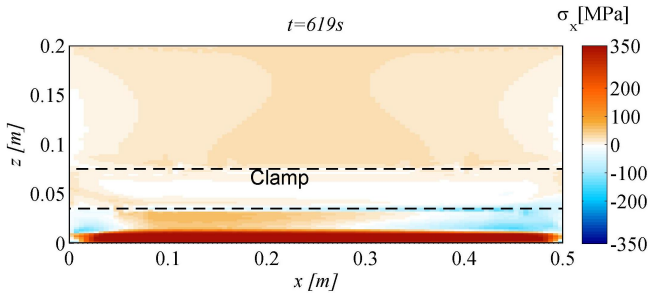

FIGURE 14. LONGITUDINAL RESIDUAL STRESS AFTER 400s OF COOLING.

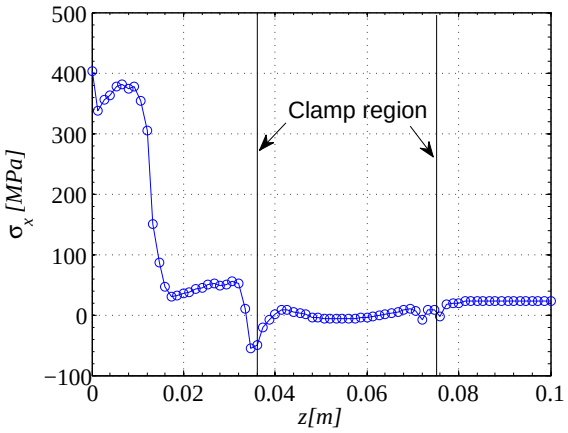

FIGURE 15. LONGITUDINAL RESIDUAL STRESS AFTER 400s OF COOLING AT A LENGTH-WISE POSITION OF 0.2m.

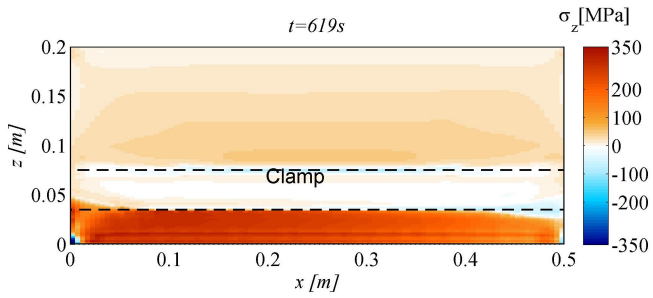

FIGURE 16. TRANSVERSE RESIDUAL STRESS AFTER 400s OF COOLING.

CONCLUSIONS

The following conclusions can be summarised from this study:

1. FEA modelling can be used without excessive computational cost by uncoupling the thermal and structural aspects to investigate the FSW process of DH36 steel. It is evident that the heat sinks and clamping configuration have a significant influence on the thermal gradient and residual stresses developed during FSW. These should be given more importance before eventually simulating the whole thermo-fluid-micro-structural phenomena.

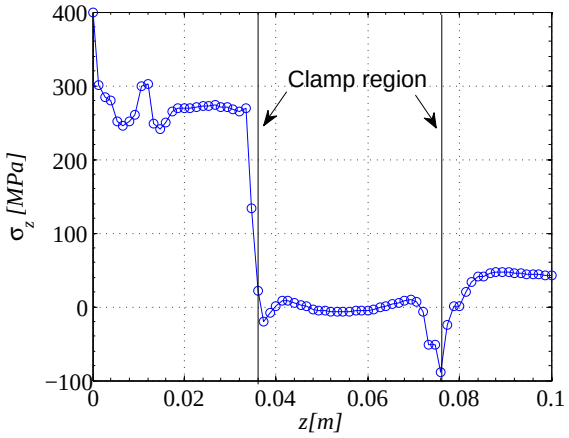

FIGURE 17. TRANSVERSE RESIDUAL STRESS AFTER 400s OF COOLING AT A LENGTH-WISE POSITION OF 0.2m.

2. At this stage a preliminary study is presented and clearly a number of experimental tests are required to validate the model and more importantly accurately establish the heat loss due to clamping. Nonetheless the assumption taken lead to a localised temperature exceeding 1000^oC at the tool region deemed to be significantly high to plasticise the weld nugget and eventually friction stir weld the assembly.
3. The heat dissipated by the clamps is low compared to the bed. Care has to be taken to ensure significant heat retention during welding but at the same time maximise heat extraction after weld completion
4. The residual stresses in the longitudinal direction exceed the yield limit of DH36 steel but are very localized to the tool region.
5. The transverse residual stresses are below the material yield limit but remain high up to the clamp region.
6. Apart from influencing the heat dissipation, the clamping configuration significantly alters the development of residual stresses thereby it is expected that they will influence the overall distortion.

This numerical analysis requires validation with experimental measurements. Such experiments will be carried out in subsequent phases of the project. Moreover, the heat input model uses an assumed friction coefficient which is as yet unknown. From these studies it is clear that the tool heat sink model is very important in determining the peak temperatures reached. This might require tuning this simplified model with either experimental or local model results. Further research is being done to understand the redistribution of residual stresses upon clamp removal. A number of optimisation models will be conducted to establish the optimal clamping and heat sink configuration.

ACKNOWLEDGMENT

This study is being funded by the European Commission in Call FP7-SST-2012-RTD-1 under the project titled High Integrity Low Distortion Assembly Hilda. The authors would also like to acknowledge the project partners in particular Mr. Stephen Cater at TWI for providing the FSW parameters and setup configuration together with Dr. Alex Galloway the project coordinator of the HILDA project. This work reflects only the authors views and the European Union is not liable for any use that may be made of the information contained therein.

REFERENCES

[1] Morris, T., David, N. E., Christopher, N. J., George, M. M., Templesmith, P., and Dawes, C. "Improvements related to friction welding". *EPO Patent EP 0615480*.

[2] Mishra, R., and Mahoney, M., 2007. *Friction Stir Welding and Processing*. Asm International.

[3] McPherson, Galloway, A., Wood, J., and Cater, S., 2012. *A comparison between single sided friction stir welded and submerged arc welded DH36 steel thin plate*. 9th International Conference on Trends in Welding Research. Chicago, June.

[4] Fratini, L., 2009. "Friction stir processing: Thermomechanical loads and consequent effects on the local material characteristics". *Proceedings of the Institution of Mechanical Engineers, Part L: Journal of Materials Design and Applications,* ***223***(1), pp. 31–39.

[5] Soundararajan, V., Zekovic, S., and Kovacevic, R., 2005. "Thermo-mechanical model with adaptive boundary conditions for friction stir welding of al 6061". *International Journal of Machine Tools and Manufacture,* ***45***(14), pp. 1577 – 1587.

[6] Staron, P., Koak, M., and Williams, S., 2002. "Residual stresses in friction stir welded al sheets". *Applied Physics A,* ***74***, pp. s1161–s1162.

[7] Riahi, M., and Nazari, H., 2011. "Analysis of transient temperature and residual thermal stresses in friction stir welding of aluminum alloy 6061-t6 via numerical simulation". *The International Journal of Advanced Manufacturing Technology,* ***55***, pp. 143–152.

[8] Zhu, X., and Chao, Y., 2004. "Numerical simulation of transient temperature and residual stresses in friction stir welding of 304l stainless steel". *Journal of Materials Processing Technology,* ***146***(2), pp. 263 – 272.

[9] Neto, D., and Neto, P., 2013. "Numerical modeling of friction stir welding process: a literature review". *The International Journal of Advanced Manufacturing Technology,* ***65***, pp. 115–126.

[10] Schmidt, H., Hattel, J., and Wert, J., 2004. "An analytical model for the heat generation in friction stir welding".

Modelling and Simulation in Materials Science and Engineering, ***12***(1), p. 143.

[11] Schmidt, H., and Hattel, J., 2005-04-01T00:00:00. "Modelling heat flow around tool probe in friction stir welding". *Science and Technology of Welding and Joining,* ***10***(2).

[12] Simar, A., Pardoen, T., and de Meester, B., 2007. "Effect of rotational material flow on temperature distribution in friction stir welds". *Science and Technology of Welding and Joining,* ***12***, pp. 324–333.

[13] John, R., Jata, K., and Sadananda, K., 2003. "Residual stress effects on near-threshold fatigue crack growth in friction stir welds in aerospace alloys". *International Journal of Fatigue,* ***25***(11), pp. 939 – 948. International Conference on Fatigue Damage of Structural Materials IV.

[14] Bussu, G., and Irving, P., 2003. "The role of residual stress and heat affected zone properties on fatigue crack propagation in friction stir welded 2024-t351 aluminium joints". *International Journal of Fatigue,* ***25***(1), pp. 77–88.

[15] Khandkar, M. Z. H., Khan, J. A., Reynolds, A. P., and Sutton, M. A., 2006. "Predicting residual thermal stresses in friction stir welded metals". *Journal of Materials Processing Technology,* ***174***(3), pp. 195 – 203.

[16] Camilleri, D., and Gray, T., 2005. "Computationally efficient welding distortion simulation techniques". *Modelling and Simulation in Materials Science and Engineering,* ***13***(8), p. 1365.